Location and Intensity Discrimination in the Leech Local Bend Response Quantified Using Optic Flow and Principal Components Analysis

Serapio M. Baca, Eric E. Thomson and William B. Kristan, Jr.

J Neurophysiol 93:3560-3572, 2005. First published 2 February 2005;
doi: 10.1152/jn.01263.2004

J Neurophysiol 93: 3560–3572, 2005.
First published February 9, 2005; doi:10.1152/jn.01263.2004.

Location and Intensity Discrimination in the Leech Local Bend Response Quantified Using Optic Flow and Principal Components Analysis

Serapio M. Baca,[1,*] Eric E. Thomson,[1,*] and William B. Kristan, Jr.[2,1]
[1]*Neurosciences Graduate Program and* [2]*Section of Neurobiology, Division of Biological Sciences, University of California, San Diego, La Jolla, California*

Submitted 8 December 2004; accepted in final form 25 January 2005

Baca, Serapio M., Eric E. Thomson, and William B. Kristan Jr. Location and intensity discrimination in the leech local bend response quantified using optic flow and principal components analysis. *J Neurophysiol* 93: 3560–3572, 2005. First published February 9, 2005; doi:10.1152/jn.01263.2004. In response to touches to their skin, medicinal leeches shorten their body on the side of the touch. We elicited local bends by delivering precisely controlled pressure stimuli at different locations, intensities, and durations to body-wall preparations. We video-taped the individual responses, quantifying the body-wall displacements over time using a motion-tracking algorithm based on making optic flow estimates between video frames. Using principal components analysis (PCA), we found that one to three principal components fit the behavioral data much better than did previous (cosine) measures. The amplitudes of the principal components (i.e., the principal component scores) nicely discriminated the responses to stimuli both at different locations and of different intensities. Leeches discriminated (i.e., produced distinguishable responses) between touch locations that are approximately a millimeter apart. Their ability to discriminate stimulus intensity depended on stimulus magnitude: discrimination was very acute for weak stimuli and less sensitive for stronger stimuli. In addition, increasing the stimulus duration improved the leech's ability to discriminate between stimulus intensities. Overall, the use of optic flow fields and PCA provide a powerful framework for characterizing the discrimination abilities of the leech local bend response.

INTRODUCTION

The ability to discriminate—to distinguish among different stimuli—is a fundamental perceptual skill (Sekular and Blake 1990). In behaviors as diverse as the visual discrimination of depth (Badcock and Schor 1985) and the tactile discrimination of touch location (Johnson and Philips 1981), organisms discriminate stimuli on spatial scales finer than the width of individual sensory receptors, a phenomenon known as hyperacuity (Churchland and Sejnowski 1992). In addition to discriminating between the same stimulus presented at different locations, increasing or decreasing a behavioral response based on stimulus intensity–known as *scaling* in the psychophysical literature–is also a fundamental feature of many sensorimotor systems (Werner 1980). Direct comparisons of neuronal and psychophysical performance have revealed neural mechanisms responsible for such exquisite discriminative abilities (reviewed by Parker and Newsome 1998).

Leech local bending, in which the body shortens near the site of light mechanical stimulation, is sensitive to both stimulus location (Lewis and Kristan 1998a) and stimulus intensity (Kristan 1982; Lewis and Kristan 1998a). For many reasons, the local bend response is a useful model for studying how neurons discriminate between stimuli. First, it is easy to record from the sensory neurons, or stimulate them, while monitoring local bending (Lewis and Kristan 1998b; Zoccolan and Torre 2002; Zoccolan et al. 2001). Second, only a small number of identified neurons produce local bending (Kristan 1982; Lewis and Kristan 1998a; Lockery and Kristan 1990a, b; Pinato and Torre 2000; Zoccolan et al. 2002). Third, the experimental preparation is simple, consisting of a single innervated segment of the body wall (Lewis and Kristan 1998b). Fourth, the local bend response can be elicited reliably and repeatedly with no training period required.

A recent series of studies used local bending to quantitatively evaluate touch location discrimination (Lewis and Kristan 1998a–c). In those studies, the behavior was monitored using electromyography (EMG). However, EMG is an indirect behavioral measure that monitors the electrical activity in muscles and does not track body-wall movements directly. Also, previous studies showed that the local bending response increases with touch intensity (Kristan 1982; Lewis and Kristan 1998b) but did not quantify the differences. The present study overcomes the previous limitations and provides direct quantitative measures of how well the leech discriminates touch location and intensity. A motion-tracking algorithm (based on calculating the optic flow between successive video frames) quantified the body-wall movements, and we used principal components analysis (PCA) to analyze the behavioral data.

METHODS

Leech care

Adult medicinal leeches (*Hirudo medicinalis*) from Carolina Biological Supply (Burlington, NC) and Leeches USA (Westbury, NY) were maintained in 5-gallon aquaria containing Instant Ocean Sea Salt (Aquarium Systems, Mentor, OH) diluted 1:1,000 with distilled, de-ionized water. The leeches were maintained in a cool room (15°C) with a 12-h light-dark cycle. Leeches ranged from 2 to 5 g, and we used leeches that had not consumed a blood meal for ≥4 wk before experimentation because preliminary observations showed local bending to be more reliably elicited in food-deprived leeches.

* Both authors contributed equally to this research.

Address for reprint requests and other correspondence: W. B. Kristan Jr., University of California, San Diego, Neurobiology Section, Div. of Biological Science 0357, 9500 Gilman Dr., La Jolla, CA 92093-0357 (E-mail: wkristan@ucsd.edu).

The costs of publication of this article were defrayed in part by the payment of page charges. The article must therefore be hereby marked "*advertisement*" in accordance with 18 U.S.C. Section 1734 solely to indicate this fact.

Body-wall preparations

Ice-cold leech saline (Muller et al. 1981) anesthetized each animal for the duration of the dissection. At the beginning of an experiment, the cold saline was replaced by room temperature saline that continuously superfused the body wall preparation. Preparations produced reliable local bends for ≥6 h when stimulating the body wall at 3.5-min intervals. Previous studies found no sensitization or habituation in motor neurons when eliciting local bending every 2 min (Lockery and Kristan 1991).

The body-wall preparations used in this study are similar to those used previously (Kristan 1982; Lewis and Kristan 1998a; Mason and Kristan 1982; Nicholls and Baylor 1968). Briefly, we dissected three segments from the leech midbody region (Fig. 1*A*), then cut the three segments along the dorsal midline. After removing the internal connective tissue and viscera, we flattened the body wall and pinned it skin-side-up on a silicone elastomer (Sylgard, Dow Corning, Midland, MI)-coated plastic petri dish (Fig. 1*B*). The anterior and posterior ganglia were removed, leaving the central segment innervated by a single ganglion. We secured the anterior and posterior edges of the body wall to the dish using 8–12 Minuten pins, but we used only 5 pins to secure the dorsal edges to minimally impede longitudinal body wall movements. This preparation produced large, replicable local bend responses similar to those in intact, unpinned preparations.

Optical recording

We recorded the image of the body-wall preparation (Fig. 1*B*) through a Wild dissection microscope using a C-Mounted Hitachi

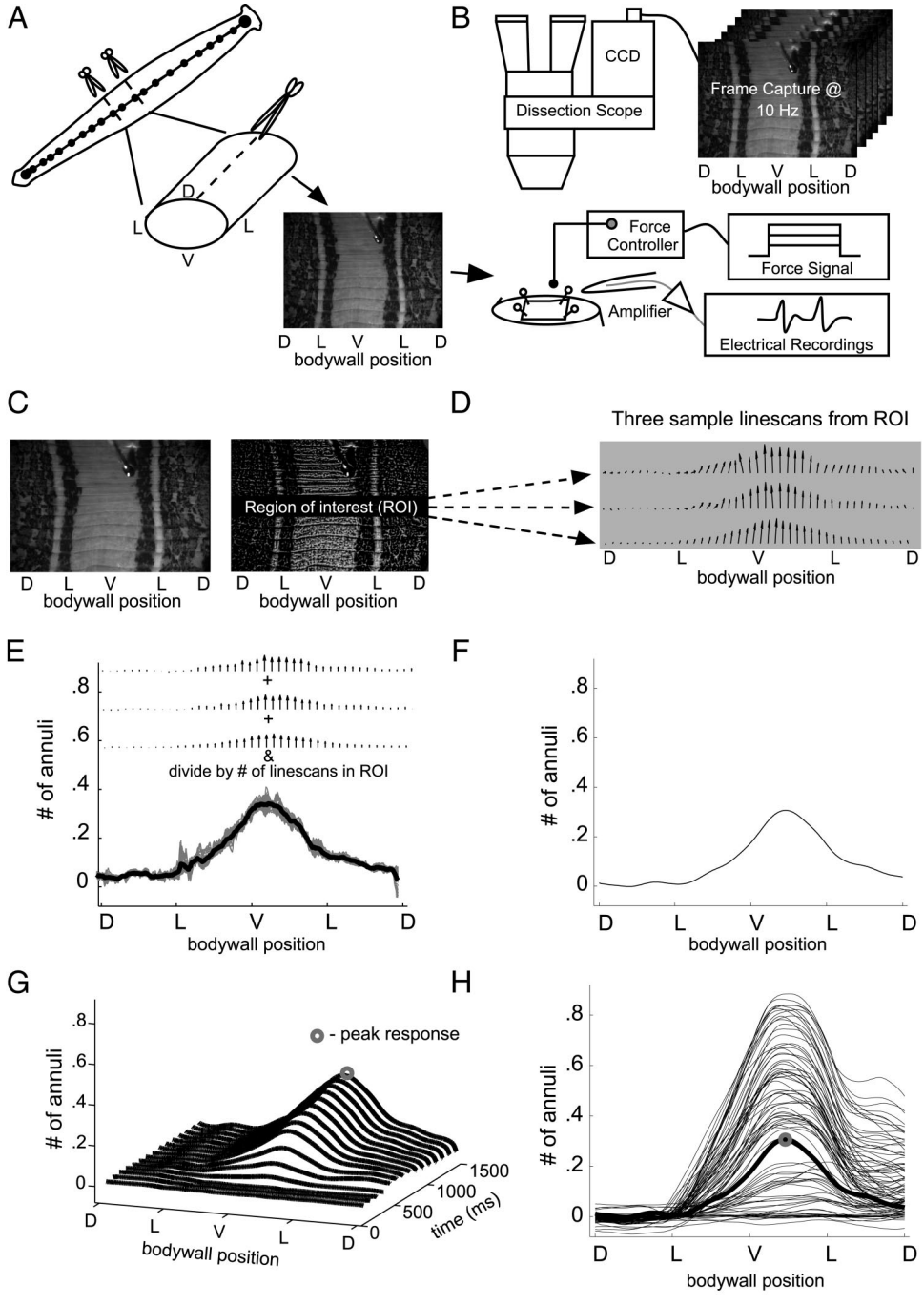

FIG. 1. The experimental preparation and experimental procedures. *A*: an intact leech has a cylindrical body that tapers at both anterior and posterior ends. Running ventrally along its long axis is its CNS; each swelling along the nerve cord corresponds to a single segmental ganglion. We used a body wall preparation consisting of 3 segments taken from the middle of the animal with the ganglion innervating the central segment being the only one left intact. After cutting along the dorsal midline, we flattened the body wall and pinned it skin-side up in a recording chamber. In this panel and many subsequent ones, the letters D, L, and V signify mid-dorsal, mid-lateral, and mid-ventral locations on the body wall, respectively. *B*: we viewed the preparation through a dissecting microscope with an attached CCD camera. Images were captured on 1 computer while the electrophysiological recordings and the signals to the force controller were captured by a 2nd computer. TTL pulses synchronized image frames with times of stimulus presentation. *C* and *D*: an adaptive histogram equalization routine increased local contrast and provided many features for subsequent tracking. Optic flow fields were calculated to determine the movement of the body wall over time from successive images collected at 10 Hz. An optic flow field region of interest (shaded in *C* and *D*) was chosen (see METHODS) and remained fixed for the duration of the experiment. *E*: for each optic flow vector in the region, we took the projection along the long axis of the animal and plotted these projections over body wall location. The gray lines are the individual traces and the black line represents the averaged values. The distance moved (*y* axis) has been divided by the average width of an annulus so that the units are number of annuli. *F*: a single local bend profile was created by smoothing the averaged distance profile with a Gaussian filter. *G*: averaged, smoothed profiles of a single response over time, sampled at 10 Hz for 1.5 s. The fifteenth profile was the first one that contained the maximal value (peak response, circle) obtained in this response. *H*: a graph of 48 peak response profiles in response to stimuli at 7 different amplitudes obtained in 1 preparation. The peak response from *G* is shown as a thick line marked with a circle at its peak.

KP-M1 monochrome CCD camera (Image Labs International, Bozeman, MT). The images (640 × 480 pixel resolution) were captured at 10 Hz and digitized using a Scion LG-3 frame grabber card and image-acquisition software (Scion Corporation, Frederick, MD) on either a PC or Macintosh computer (Fig. 1*B*). On a different computer, 5-V TTL pulses from AxoGraph 4 or Clampex 8 software (Axon Instruments, Union City, CA) synchronized video acquisition with the stimulus controller and the electrical recordings. Image capture lasted for 2–2.5 s and began 0.5 s before stimulus presentation for a total of 20–25 images/trial.

Stimulus: force controller

Previous studies of the local bend response have applied pressure to the leech using solenoid-driven nylon filaments (von Frey hairs) (Lewis and Kristan 1998b; Zoccolan and Torre 2001). Despite their utility, von Frey hairs have several shortcomings: on a given trial, there is no way to monitor the *actual* force delivered; the force applied by a von Frey hair varies with the humidity and, to a lesser degree, temperature of the filament (Andrews 1993); to vary touch intensity, one must switch filaments because a given hair produces only one force intensity; and the filaments that produce different forces have different cross-sectional areas, so it is not possible to control force and surface area independently. To overcome these difficulties, we used a Dual-Mode Lever Arm System (Aurora Scientific, Ontario, Canada, Model 300B) to deliver specified force waveforms to the leech body wall (Fig. 1*B*). The force controller takes a user-defined time-varying voltage signal as input and, within 1.3 ms, its lever arm produces forces from 0 to 500 mN, as determined by an input voltage signal (50 mN/V). A feedback loop keeps the delivered force within 1 mN of the desired level.

We stimulated the skin of the leech with a 28-gauge needle that had a small (~1 mm^2 diam) bead of epoxy on its tip (Fig. 1*B*). The head stage of the force controller was mounted on a micromanipulator (Narishige International, East Meadow, NY). We used AxoGraph 4 or Clampex 8 to generate waveforms that produced force steps of varying duration and intensity. The forces delivered were monitored using the same programs, and we eliminated those trials in which the measured force deviated from the desired force by >5%; this occurred on ~3% of all trials.

Our mechanical stimulator had a much larger cross-sectional diameter (1 mm) than the von Frey hairs used in previous studies (Lewis and Kristan 1998b). Hence to be sure that our stimuli produced comparable effects to those used in previous studies, we chose our stimulus range to correspond to that which would produce similar P cell (the mechanoreceptors mainly responsible for the local bend response) spike counts to those observed in studies using the smaller-diameter von Frey hairs (Kristan 1982; Lewis 1999; Lewis and Kristan 1998a; Zoccolan and Torre 2002; Zoccolan et al. 2001, 2002).

Image processing and analysis

ADAPTIVE HISTOGRAM EQUALIZATION. To use optic flow for tracking movement of the leech body wall over time requires feature-rich images (Zoccolan et al. 2001). The dorsal body wall is richly patterned, but the ventral surface is more uniform in texture and color (Fig. 1*C*). To reveal distinguishable features in the ventral region, we processed each image with an adaptive histogram equalization (AHE) routine implemented in an Adobe Photoshop plug-in (Reindeer Graphics, Asheville, NC). The AHE algorithm enhances local image contrast by scaling pixel intensities to use the full scale of possible pixel intensities in localized regions of the image, thereby increasing contrast. AHE has been used to reveal important anatomical details in a variety of biological tissues (Buzuloiu et al. 2001; Morrow et al. 1992; Paranjape et al. 1992, 1994;), and we observed significant improvements in tracking ventral body wall movements after AHE processing. We tuned the AHE parameters using one body wall preparation, and then we used the same parameters for all the preparations because all leech body wall had similar patterning. The increase in distinctive features in the ventral region can be seen by comparing the unprocessed and processed images in Fig. 1*C*.

OPTIC FLOW ANALYSIS. Previous studies introduced a correlation-based optic flow algorithm to characterize leech body-wall movements from video recordings (Zoccolan and Torre 2002; Zoccolan et al. 2001, 2002). We used a different, gradient-based algorithm (Lucas and Kanade 1981) that produces a very dense optic flow field for each pair of images. This algorithm provides very accurate motion estimations over a wide range of conditions (Barron et al. 1994). We used the optic flow algorithm in conjunction with a course-to-fine framework to improve the motion estimates (Beauchemin and Barron 1995; Bergen et al. 1992). Briefly, the full size images (640 × 480 pixels) are scaled down (i.e., 320 × 240 and 160 × 120 pixels), effectively producing spatially averaged image sequences. The OF algorithm is applied to these "sub-sampled" images to produce gross motion estimates. These estimates are then used to constrain the motion estimates made on the full-size image sequence, producing more uniform optic flow fields and reducing the likelihood that local pixel noise will result in poor tracking. The optic flow code was written in ANSI C by Dr. Ming Ye (Ye and Haralick 2000). We obtained similar but denser optic flow fields compared with those generated previously (Zoccolan et al. 2001) when we tested both algorithms on the same body-wall image sequence.

BEND PROFILE CALCULATION. For each trial, we captured images at 10 Hz for 2.0–2.5 s. These 20–25 frames spanned the time before, during, and after stimulation. We applied the AHE routine to each image in the sequence, then calculated optic flow fields between successive frames (i.e., the 2nd image was compared with the 1st; the 3rd was compared with the 2nd, etc.). After calculating the movements of the entire body wall, we selected a rectangular region of interest (ROI) that showed robust movement and was free from edge or pinning artifacts (Fig. 1*C*). The ROI spanned one to two annuli along the long axis of the leech and included its entire circular axis. (An annulus is a raised ring of the leech body wall; there are 5 annuli per body-wall segment.) For a given leech, the selected region remained fixed for all trials.

Within the ROI, we monitored movements produced primarily by the longitudinal muscles, which shorten the longitudinal axis of the body wall (Stuart 1969, 1970). Hence, for each pixel in the ROI, we extracted the component of the movement that ran parallel to the leech's long axis. The average movement at each circumferential location in the ROI created a profile of longitudinal movement between any two images (Fig. 1, *E* and *F*). We smoothed these motion profiles with a Gaussian filter. For each trial, we calculated these motion profiles at each time point, generating a three-dimensional characterization of the local bend over time (Fig. 1*G*). Because the movement peaked at ~1.5 s after stimulus onset and held steady for some time, we used the motion profile at 1.5 s to represent the bending response and called this the *bend profile*. Figure 1*H* shows the set of 48 bend profiles obtained from a single body wall in response to stimuli at the same location but of varying intensities.

We eliminated "outlier" bend profiles, defined as those that contained obviously impossible deformations of the body wall or those in which the SE of the optic flow field exceeded three pixels (a single annular ring is 20–40 pixels wide). Viewing the original video frames, outliers always had obvious and technical problems such as water splashing in the dish or large variations in the illumination intensity.

Formally, bend profiles (Fig. 2, *A* and *B*) are M-element vectors, in which M is the number of pixels around the circumference of the body wall. M varied between 400 and 640, depending on the magnification used and the size of the leech. The units used for displacement in bend profiles were originally pixels, which were then normalized to the number of pixels per annulus for each leech so that all displacements were ultimately measured as numbers of annuli. We converted the units used to measure circumferential location from pixels to degrees

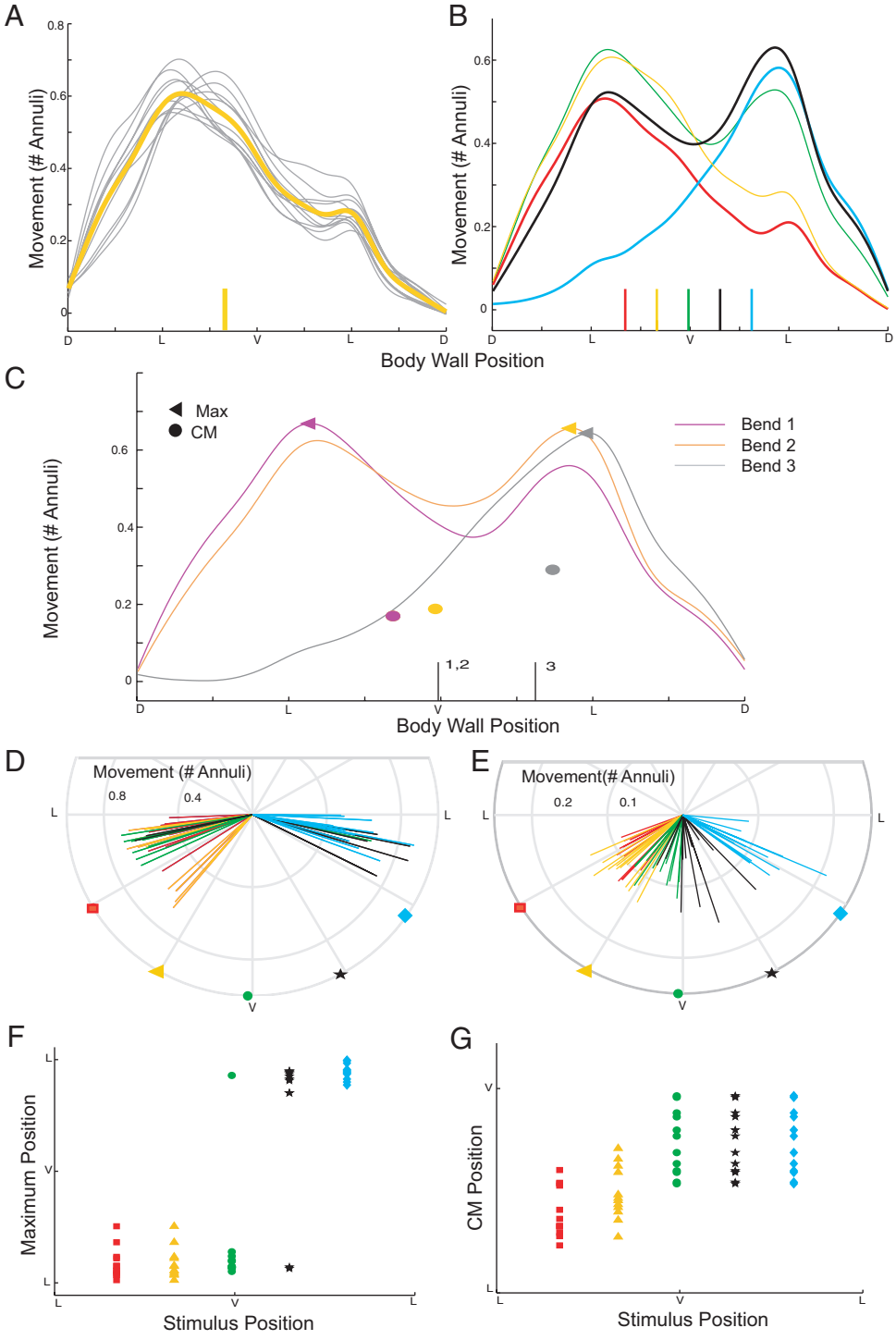

FIG. 2. Using response maximum (Max) and center of mass (CM) to quantify local bending responses. *A*: a representative example of trial-by-trial variability in the local bending response profiles. The 12 lines are individual responses to stimuli delivered at the single location marked on the abscissa. The stimulus was a force step of 200 mN lasting 200 ms. The thick yellow line is the mean of the responses. *B*: mean response profiles to stimuli at the 5 locations marked on the abscissa. The touch locations are 108, 144, 180 (the ventral midline), 216, and 252°. The colors of the traces correspond to the colors of the markers that indicate the touch location. *C*: Max and CM of the local bending response. Two of the response profiles (1 and 2) were generated by stimuli at the ventral midline (at 180°); the 3rd response was generated by stimulating at site 3, to the right of the ventral midline (at 257°). The maxima are marked with triangles. The centers of mass are marked with circles whose colors match the colors of the appropriate line. *D*: polar representation of profile Max for 60 trials from 1 experiment. The responses are color-coded by stimulus location, which are marked on the circular axis. *E*: polar representation of profile CM for the same 60 trials as *D*. The color coding is the same as *D*. *F* and *G*: cartesian representations of profile maxima and centers of mass for the same experimental data presented in *D* and *E*. The color coding for stimulus position is the same as *D*.

by setting the pixel at the left edge of the dorsal body wall to 0°, the pixel at the ventral midline to 180°, the one at the right edge of the dorsal body wall to 360°, and fitting a line to these three points. The movement at pixel i can be represented in polar coordinates as

$$z_i = (\theta_i, R_i)$$

where R_i is the magnitude of the movement at location θ_i. The movement at pixel i was sometimes represented in Cartesian coordinates using $\bar{x}_i = (x_i, y_i)$, which describes the x and y components of the bend at pixel i ($x_i = R_i \cos\theta_i$ and $y_i = R_i \sin\theta_i$).

Quantifying responses: four methods

We used four methods to get compact descriptions of the high-dimensional bend profiles.

MAXIMUM. The maximum is the location (in degrees) and magnitude (in number of annuli) of the peak of the bend profile (Fig. 2*C*).

CIRCULAR CENTER OF MASS. The circular center of mass $\bar{V}$ (Fig. 2*C*) is the vector sum of the movement over all M pixels divided by the total number of pixels

$$\bar{V} = \frac{\sum_{i=1}^{M} \bar{x}_i}{M}$$

where $\bar{x}_i$ is the Cartesian representation of the displacement at pixel i.

COSINE. We fit the local bend profile with a cosine of the form

$$C(\theta) = A \cos(\theta - \omega) + S$$

where A is the amplitude of the cosine, ω is the phase, and S is the vertical shift. The maximum of the best-fit cosine is at position ω and the magnitude at its peak is $A + S$. We fit our data to $C(\theta)$ using a nonlinear least-squares algorithm implemented by Matlab's *lsqcurvefit* function (Fig. 3*A*). This is similar to the cosine fit used previously (Lewis and Kristan 1998b) although we use an additional free parameter for amplitude: in the previous study the data were normalized so that the maximum was unity.

As in a previous study (Lewis and Kristan 1998b), we eliminated all trials that had <65% of their variance explained by the cosine fit (Fig. 3*B*). The percentage of the variance explained on trial i is

$$P(i)_{\text{fit}} = 100\left(1 - \frac{\text{SSE}_{\text{fit}}}{\text{SSE}_{\text{data}}}\right) \quad (1)$$

where SSE_{data} is the sum of the squared deviations of the data from the mean of trial i, and SSE_{fit} is the sum of the squared deviations of the data from the best cosine fit for the trial.

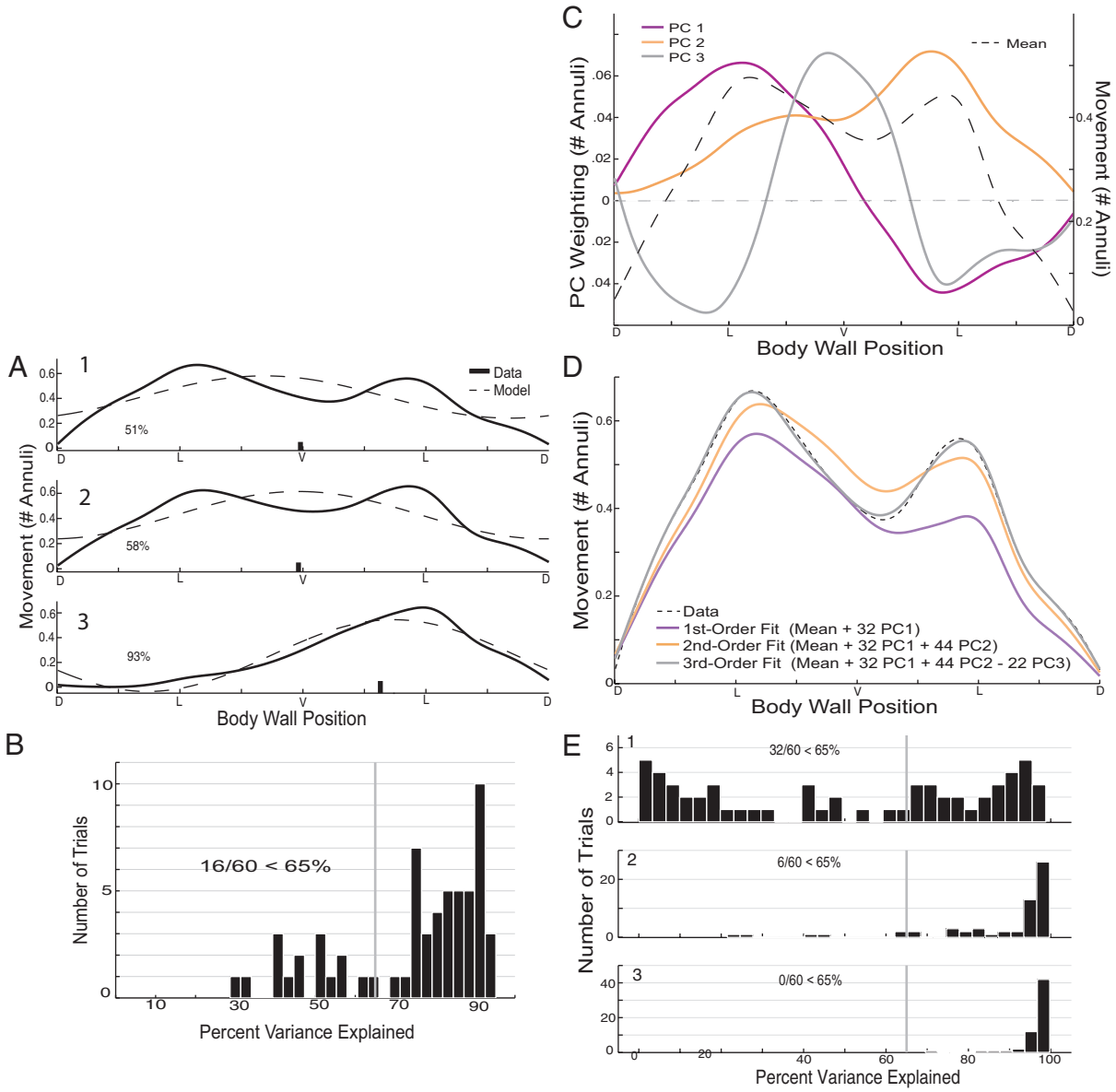

FIG. 3. Comparing principal component analysis (PCA) and cosine fits as measures of local bending responses. *A*: cosine fits to the 3 bend profiles (*1–3*). The cosine fits accounted for 51, 58, and 93% of the variability in the data, respectively. The marks on the abscissa indicate the touch locations. *B*: histogram of the percentage of variance explained using the cosine fit on 60 response profiles. Sixteen of the fits (27%) were judged to be poor because they accounted for <65% of the variability. *C*: —, the 1st 3 principal components (PCs), color-coded, that were extracted using PCA as described in the text. dark - - -, the mean of the 60 bend profiles (the same as for *B*) used to generate the PCs. *D*: an example of the fitting procedure. The fitted profile became closer and closer to the original bend profile (dark - - -) by progressively adding scaled copies of the 1st 3 principal components (PCs) to the mean bend. The variance explained by the 1st-order fit is 74%, by the 2nd-order fit is 94%, and by the 3rd-order fit is >99%. *E, 1–3*: histograms of the percentage of variance explained by the 1st-, 2nd-, and 3rd-order fits, respectively for the same 60 bend profiles used in *B*.

PCA. PCA is a quantitative technique that simplifies the visualization and analysis of high dimensional datasets (Jackson 1991). We used PCA to reduce the number of parameters needed to represent the bend profiles. Given the set of all M-dimensional bend profiles from an experiment, PCA generates a set of M-dimensional bend profile components, called the *principal components* (PCs) of the data (e.g., Fig. 3*C*). Every trial in the original dataset can be reconstructed, or fit, by a weighted sum of n PCs. This nth-order fit of trial i, F_i^n, is calculated as

$$F_i^n = \mu + \sum_{k=1}^{n} \alpha_{ik} \mathrm{PC}_k \qquad (2)$$

where μ is the mean of all bend profiles (i.e., the *mean bend profile*), and α_{ik} is the weight, or *score*, of PC_k for trial i. Figure 3*D* shows one such mean bend profile from an experiment as well as the first-, second-, and third-order fits of one bend profile from the same experiment. The PCs were obtained by diagonalization of the covariance matrices of the data sets using the *princomp* function in Matlab.

PCs are ordered such that PC_1 accounts for more variance in the data set than PC_2, PC_2 accounts for more variance than PC_3, and so on (Jackson 1991). In *Eq. 2, n,* the number of PCs used to reconstruct the data, must be determined. We used the number of PCs required to ensure that ≥65% of the variance in every profile was explained. The percentage of the variability explained on a given trial was calculated using *Eq. 1,* where $\mathrm{SSE}_{\mathrm{data}}$ is the sum of the squared deviations of a given trial from μ, the mean bend profile. In all experiments performed in this study, this criterion was met by using three or fewer PCs (i.e., $n \leq 3$) to fit the data.

Once PCA was performed on the bend profiles from a data set, the individual bend profiles could be represented as vectors containing the first n PC scores, where n is the highest order used in *Eq. 2.* Because our data could be reconstructed using a low (i.e., 1st, 2nd, or 3rd)-order fit, this representation of bend profiles in *score space* greatly eased visualization and statistical analysis of the bend profiles (Fig. 4*B*).

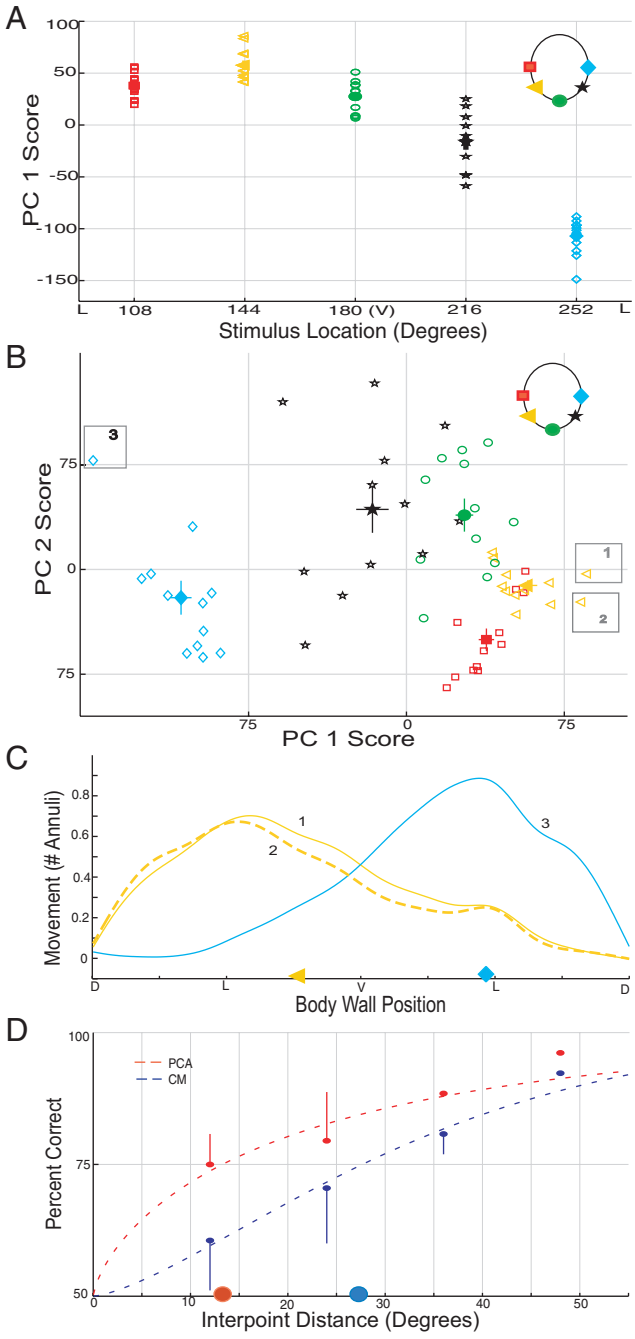

FIG. 4. Using PC scores to track touch location. *A*: plot of PC_1 scores as a function of touch location. The responses are color-coded by stimulus location, as indicated on the body wall icon in the *top right corner* of *B*. Filled symbols, means; unfilled symbols, individual responses. PC_1 scores were strongly negatively correlated with touch location ($r = -0.84$). *B*: scatter plot of PC_2 versus PC_1 scores for the same 60 observations. Unfilled symbols, individual trials; filled symbols, means ± SE. The colors and symbols correspond to the responses shown in *A*. The original bend profiles corresponding to the 3 boxed observations are shown in *C*. *C*: 3 bend profiles highlighted in *B,* illustrating that the PC representation of profiles preserves the similarities and differences among the original profiles. The touch locations are indicated by color on the abscissa. *D*: discrimination performance the body-wall preparation. Six preparations were stimulated 12 times at each of 5 locations [156, 168, 180 (the ventral midline), 192, and 204°] that were 12° apart. The graph plots percent correct as a function of distance between touch locations. Solid circles, the mean performance (±SE) of the classifier; the dotted lines, best fits to the data points. The red line and data points are measures when the 1st 3 PC scores are used to represent the behavioral response, and the blue line and data points are the measures obtained using center of mass to represent the response. Filled circles on the abscissa, the threshold values, $\Delta_{75}(S)$, obtained using the 2 different measures (i.e., ~14° for PCA and ~27° for CM).

Quantifying stimulus discriminability

To quantify how well the leech discriminated touch location, we used a *classifier* to determine the segregation between the response distributions to touches at two touch locations at different stimulus distances, $\Delta\theta$ (Fig. 4*D*). A classifier is a mathematical function that estimates which stimulus was presented based only on the behavioral response (Duda et al. 2000). The percentage of correct stimulus classifications depends on the degree of overlap of the response distributions to the stimuli: if response distributions are completely segregated, a good classifier will be correct on 100% of the trials; if the distributions completely overlap, a good classifier will perform at chance (50% correct in the 2-stimulus case) (Duda et al. 2000; Thomson and Kristan 2005). We used a *nearest-neighbor classifier* (Duda et al. 2000), which classifies the stimulus that produced the response on trial i as the same as the stimulus that generated the nearest-neighbor response, using Euclidean distance. The stimulus estimate is correct when the nearest response was evoked by the same stimulus and is incorrect when the nearest response was evoked by a different stimulus.

The *threshold touch-location increment*, $\Delta_{75}(\theta)$ (sometimes called the *just noticeable difference or JND*), is the distance between two stimuli at which the classifier is 75% correct. $\Delta_{75}(\theta)$ is a standard measure of threshold; for the two-stimulus case, it is halfway between chance and perfect performance (Johnson and Philips 1981). We

obtained $\Delta_{75}(\theta)$ estimates from "psychophysical" curves that plot percent correct versus the distance between stimulus locations (Fig. 4*D*). We generated such curves in three steps. First, we applied a nearest-neighbor classifier to the set of responses to two different stimuli (e.g., Fig. 4*B,* squares and circles) to calculate percent correct for a series of response pairs with inter-touch distances of 12, 24, 36, and 48° (Fig. 4*D*). Second, we fit each set of percent correct values with a saturating exponential function constrained within a minimum of 0.5 (discrimination at chance) and a maximum of 1.0 (perfect discrimination)

$$P_c(\Delta\theta) = 1 - 0.5 \exp[-(\Delta\theta/\gamma)^{\beta}] \quad (6)$$

where $\Delta\theta$ is difference in touch location distance, γ is the value of $\Delta\theta$ at which the curve has increased to 64% of its maximum, and β is the slope of the curve at that point. Third, we used the best fit of *Eq. 3* to calculate the threshold inter-touch distance, $\Delta_{75}(\theta)$.

We used a different, parametric method to quantify the *threshold touch-intensity increment*, $\Delta_{75}(I)$, where I is touch intensity. Because the local bend response was a nonlinear function of touch intensity (Fig. 5*C*) and discrimination is better at steeper slopes, we needed to calculate the threshold touch intensity increment as a function of touch intensity. If there is a linear relationship between a stimulus and the mean response to that stimulus (Fig. 5*B*), the threshold touch intensity increment is

$$\Delta_{75}(I) = 2\text{cumgauss}^{-1}(0.75, \sigma_R)/m \quad (4)$$

where m is the slope of the function relating touch magnitude to the mean behavioral response, σ_R is the SD of the responses, and $\text{cumgauss}^{-1}(p,\sigma_R)$ is the inverse cumulative distribution function of a Gaussian with SD σ_R and mean of 0. If p is a value between 0 and 1, $\text{cumgauss}^{-1}(p,\sigma_R)$ calculates the response (r) in the set of all possible responses (R) such that $P(R \leq r) = p$, where R has a Gaussian distribution with SD σ_R and mean 0 (Larsen and Marx 2000). Note that the applicability of *Eq. 4* assumes each response distribution is Gaussian with a SD σ_R (see APPENDIX for more details).

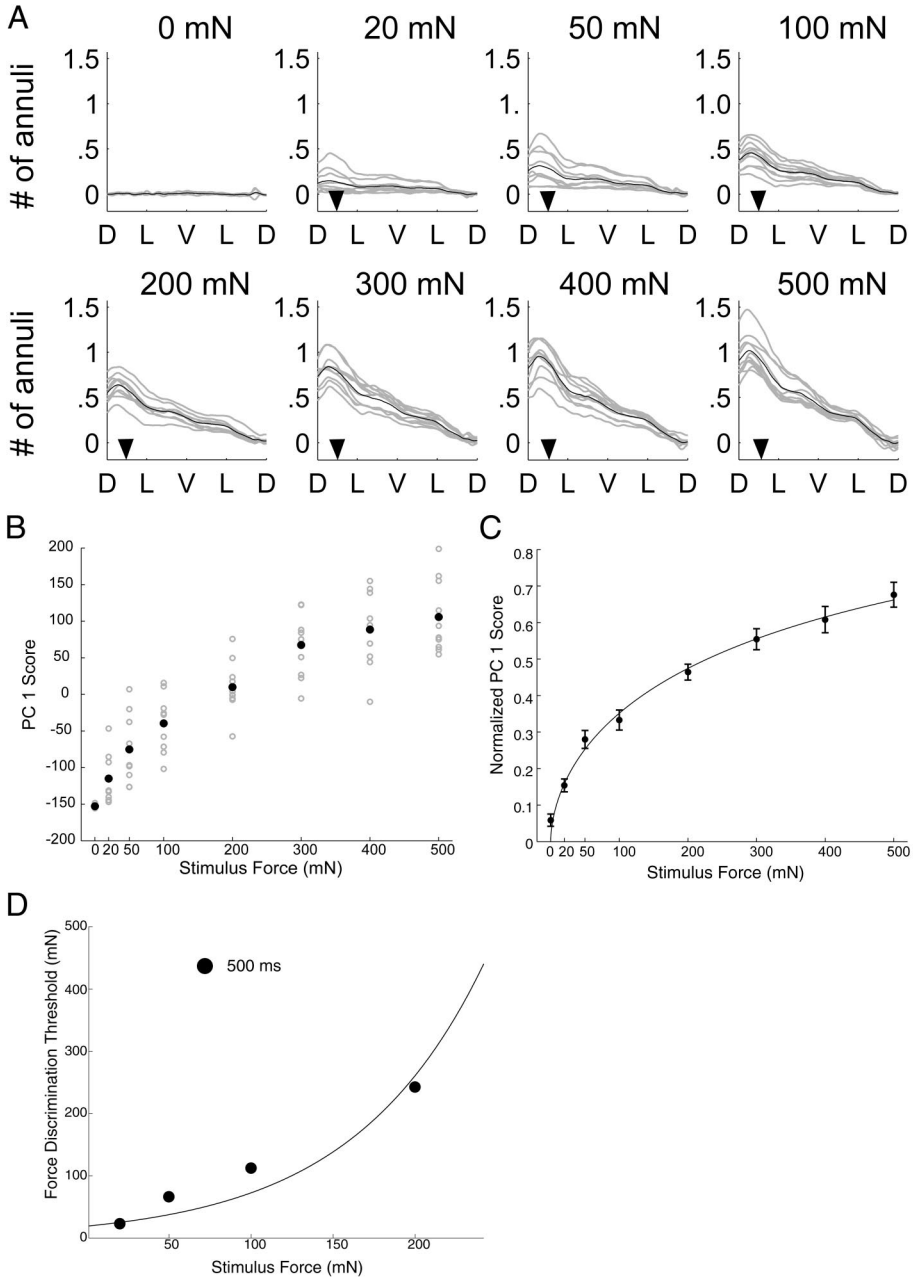

FIG. 5. PCA scores reflect changes in local bend amplitudes evoked by different force intensities at a single touch location. *A*: local bend profiles at a single site in a single preparation. We elicited 12 bends at each of 8 stimulus intensities between 0 and 500 mN for 500 ms in random order. Trials with no measurable response were included. Individual trials are represented by gray lines and the mean responses by black lines. The arrows mark the stimulus position on the body wall. *B*: PC_1 score for each local bend profile grouped by force intensity. Individual trials are represented as gray circles and the mean score at each stimulus force is in black. *C*: pooled PC_1 scores for 4 leeches. The curve is a simple exponential fit to the data (see APPENDIX). *D*: the force discrimination threshold, $\Delta_{75}(S)$, derived from the data in *C*. Discrimination of stimulus force was best at the lower intensities (20–250 mN).

According to *Eq. 4,* the steeper the slope of the function relating touch intensity to response, the lower the threshold touch intensity increment (i.e., the better the discrimination). To understand this relationship, consider two extremes. First, as m goes to zero, the threshold increment goes to infinity: all stimuli evoke the same response and the organism cannot discriminate between stimuli. Second, if the slope of the relationship is very steep, even very small changes in the stimulus will evoke different responses.

Equation 4 was used to calculate the *instantaneous threshold touch intensity increment*. Because the curve relating touch intensity to response was nonlinear (Fig. 5*C*), we calculated $\Delta_{75}(I)$ as a function of the slope of that curve (Fig. 5*D*). That is, given a slope m and SD σ_R of the curve, it is possible to calculate what the threshold touch intensity increment would be *if the response had that slope at every intensity*. To calculate m we first fit the PC_1 scores for each stimulus force with a simple exponential function

$$PC_1(I) = A(B - \exp(I/C) \quad (5)$$

where the function has an asymptote at AB and a y intercept at $A(B - 1)$. The curve is overlaid on the mean PC_1 scores in Fig. 5*C*. Second, we calculated the derivative m of the best fit to *Eq. 5* at each touch intensity. Because σ, the SD of the response, increased linearly with touch intensity (Fig. 5*C*), we fit a straight line through these points. We inserted the estimates of m and σ_R from this line into *Eq. 4* to estimate the *threshold touch intensity increment*, $\Delta_{75}(I)$, as a function of stimulus intensity.

We used *Eq. 4* to compare our estimates of touch-location discrimination to previous estimates that used the root-mean-squared (RMS) distances between touch locations and the locations of the peak EMG response (Lewis and Kristan 1998b). RMS error is an estimate of the SD of a random variable (Zar 1999); because the responses had a Gaussian distribution, *Eq. 4* applies.

RESULTS

Qualitative features of the local bend

In six body-wall preparations, we stimulated 8–13 times at five locations spaced 36° apart at circumferential intervals along the ventral surface of the body wall. We used a 200-mN force step that lasted 200 ms. The behavior was characterized by a *bend profile* that describes the net displacement of the body wall in the longitudinal direction 1.5 s after the onset of the stimulus (METHODS). Figure 2*A* shows the mean and individual bend profiles obtained when we delivered 12 stimuli at the same location. Figure 2*B* shows the mean response for this location as well as the mean bend profiles at four other touch locations. These representative results show that each touch location along the ventral surface produces a bend profile with two peaks located near the lateral edges. This bimodality was not previously reported (Lewis and Kristan 1998a), probably because previous techniques sampled fewer locations.

Comparing methods for quantifying behavior

To quantify how well the leech discriminates touch location and intensity, we needed to measure the responses on individual trials. To find the best method, we compared four ways to summarize the bend profiles: maximum, center of mass, cosine fit, and PCA.

MAXIMUM. We first represented the bend profiles using the location and magnitude of their maxima (Fig. 2*C*). A polar plot of the maxima from one experiment (Fig. 2*D*) shows that the maximal values segregate into two clusters. This pattern was seen in five of the six preparations. This bimodal clustering directly reflects the two peaks in the bend profiles (Fig. 2*B*). The relative heights of these peaks varied with touch location, so that the measured maximum was whichever of the two peaks was larger. The details of the clustering in Fig. 2*D* indicate some stimulus-dependent segregation: the stimuli to the left of the ventral midline produced peak responses near the left lateral edge, and stimuli to the right produced peak responses on the right side (Fig. 2*F*). This preparation showed a left-side bias: stimuli on the ventral midline tended to produce larger responses on the left side.

CIRCULAR CENTER OF MASS. Using center of mass to represent response location (Fig. 2*C*) produced a broader range of responses (Fig. 2*E*). Qualitatively, this measure tracked the stimulus well: the clusters of response vectors in Fig. 2*E* progress from left lateral edge through the ventral midline to the right lateral edge in the same order as the stimulus progression (Fig. 2*G*). (This measure, too, showed the leftward response bias in this experiment: the responses tended to be clustered to the left of the stimulus site). We next calculated whether the center of mass tended to be centered at the location of touch. We pooled the centers of mass from all six experiments after normalizing response amplitude to the maximum in each experiment. For four of the five touch locations, the mean location of the center of mass was found to be significantly different from the stimulus location ($\alpha = 0.05$, V test) (Zar 1999).

Although the center of mass proved to be a more useful summary of the local bend response than the maximum, it leaves out the spatial detail of the bend profiles. To capture such detail, we evaluated two methods that explicitly represent the entire bend profile: cosine fits and PCA.

COSINE FITS. In a previous study, a cosine was fit to EMG responses to touch stimuli measured at four locations along a relatively narrow (135°) band of the leech body wall (Lewis and Kristan 1998b). The cosine fit proved to be below criterion (65% of the variance explained) in more than a third of the trials in that study, but these poor fits might be improved by applying our more sensitive optic flow measurements. We explored this possibility by fitting cosines to the bend profiles generated by optic flow.

Using nonlinear least squares, we fit each bend to a cosine. Such a fit for three individual bend profiles in a single preparation, stimulated twice at the same mid-ventral location and once more laterally (Fig. 3*A*), shows that a cosine provided a poor fit to the responses in Fig. 3*A, 1* and *2,* explaining only 51 and 58% of the variance, respectively. Over all trials in the experiment, 16 of the 60 fits explained <65% of the variance (Fig. 3*B*). Over all six experiments, 20% of trials had to be rejected by the 65% criterion. This is better than the 35% rejection rate obtained using EMG recordings (Lewis and Kristan 1998b), but it is still a large percentage of the data.

PCA. We used the bend profiles from each preparation to generate a set of principal components, PCs (Fig. 3*C*). The PC shapes in Fig. 3*C* are representative of the results seen when the leech was touched at multiple locations; e.g., PC_1 was typically sinusoidal with a zero crossing near the ventral midline, whereas PC_2 had two positive peaks that were closer together than the peaks for PC_1.

We fit each bend profile with a weighted sum of the PCs (Fig. 3*D*): the first-order fit is the mean plus a scaled copy of PC_1, the second-order fit is the first-order fit plus a scaled copy of PC_2, and the third-order fit is the second-order fit plus a scaled copy of PC_3. The scaling factors of the PCs are called *scores.* For example, in Fig. 3*B*, the PC_1 score is 32, the PC_2 score is 44, and the PC_3 score is −22. (A negative value means that the PC curve was reflected about the *y* axis before it was summed with the other values.) For the trial shown, the third-order fit is nearly indistinguishable from the actual bend profile. For all 406 trials in six experiments, (Fig. 3*E*, *1–3*), the first-, second-, and third-order PCs accounted for >65% of the variance in all but one trial. Comparing Fig. 3, *E3* and *B,* shows that PCA with three free parameters provided a much more accurate representation of the bend profiles than did cosine fits, which also had three free parameters. Hence, for all the experiments on touch-location discrimination, we used the scores of PC_1, PC_2, and PC_3 to represent each bend profile.

PC scores vary with stimulus location

We found that, qualitatively, PC_1 scores closely track the stimulus: when the leech is touched to the left of the ventral midline they tend to be positive, and when the leech is touched to the right they tend to be negative (Fig. 4*A*). Quantitatively, stimulus location and PC_1 score showed a strong negative linear correlation ($r = -0.84$). In fact, the PC_1 scores distinguished the responses to stimuli presented near the right lateral edge (blue diamonds at 252° in Fig. 4*A*) from all other locations; i.e., these PC_1 scores do not overlap with any of the scores from the other locations. The scores at 216° are less completely distinguished from stimuli delivered at 108 and 180°, and there is significant overlap among the scores for 108, 144, and 180°.

We found, not surprisingly, that using PC_1 along with PC_2 helped to make finer distinctions (Fig. 4*B*). Responses to the same stimulus clustered together in *score space* in the PC_1 versus PC_2 plots, and clusters for different stimulus locations tended to be separate. For instance, the responses from touches to location 180° (green circles) were completely separated from those at 108° (red squares). The responses at 144° still overlapped with both the 108 and 180° responses but less than when using PC_1 scores alone. For this example, the five locations were separable by the $\Delta_{75}(\theta)$ criterion (see following text) by using just the PC_1 and PC_2 scores, without using the PC_3 scores at all. In many cases, however, using PC_3 scores did produce finer distinctions, so we usually used all three scores.

The bend profiles with markedly different PC scores were very different from one another, whereas those with similar PC scores were quite similar (Fig. 4*C*). In this example, the bend profiles for points 1 and 2 in Fig. 4*B* had nearly identical movement profiles (Fig. 4*C*), whereas point 3 had a very different profile. This specific example illustrates the general feature of PCA that PC score space preserves the distance relations among individual observations (Jackson 1991).

The experiments described so far examined the response to ventral stimulation exclusively. To determine the generality of our results, we repeated the experiments, stimulating the leech at five locations along the dorsal midline ($n = 2$) and lateral edge ($n = 2$). The PCs in these cases had the same qualitative shape as in the experiments on the ventral surface (data not shown).

Discrimination of touch location

We measured how far apart two stimuli needed to be for the leech body wall to produce different responses measured by their *two-point discrimination* (i.e., *threshold touch-location increment*), $\Delta_{75}(\theta)$. We delivered 200-mN stimuli for 200 ms to the skin at five locations separated by just 12° along the ventral surface in six preparations ($n = 6$). We chose a 200-ms duration because a previous study found that P cells delivered all their information about touch location within 200 ms of stimulus onset (Lewis and Kristan 1998a). This experiment tested whether leech *behavior* could discriminate such short stimulus durations. In one example (Fig. 4*D*), we show the best-fit lines for the two best measures of PCA (red) and center of mass (blue). In this and all other cases, we measured a finer two-point discrimination between two stimuli [$\Delta_{75}(\theta)$ was, on average, 7.8° less] for PCA than for center of mass. The mean two-point threshold using PCA was 18.7 ± 4.7°, corresponding to an absolute distance of ~1 mm in a leech 2 cm in circumference.

Discrimination of stimulus intensity

Previous studies, using force transducers and EMG signals (Kristan 1982; Lewis and Kristan 1998a–c), showed that the amplitude of the local bending response increases at greater stimulus intensities. We confirmed this qualitative finding using optic flow-derived bend profiles and PCA (Fig. 5*A*). This analysis also allowed us to determine quantitatively how well leeches discriminate between stimuli of different magnitudes at a single location. These bend profiles show a clear increase in response amplitude with increased stimulus intensity, a relationship reflected in the PC_1 score for these trials (Fig. 5*B*). Because the bend profiles at different intensities were so similar in shape, only PC_1 was needed to fit the profiles accurately.

To compare data across leeches, we normalized each PC_1 score to the maximal score in each leech (Fig. 5*C*). The curve in Fig. 5*C* is the best exponential fit to the pooled data. The steeper slope at lower force intensities means that the leech discriminates intensity better at lower intensities. This dependence of the touch magnitude threshold on stimulus intensity is quantified in Fig. 5*D*, which plots the *threshold touch-intensity increment*, $\Delta_{75}(I)$, versus touch intensity (see METHODS). This plot means, for example, that because a stimulus force of 50 mN has a threshold increment value of ~40 mN, stimuli needed to be ≥90 mN to be distinguishable from responses elicited by 50-mN stimuli and that a stimulus needed to be >490 mN to be distinguishable from a response to a 200-mN stimulus. The stimulus set covers the dynamic range of local bending because stimulus forces >500 mN damage the leech body wall and activate nociceptive (N) neurons, which produce writhing responses rather than local bending.

Stimulus duration affects the discrimination of stimulus intensity

Varying stimulus duration and examining how discrimination performance is affected provides insight as to how long

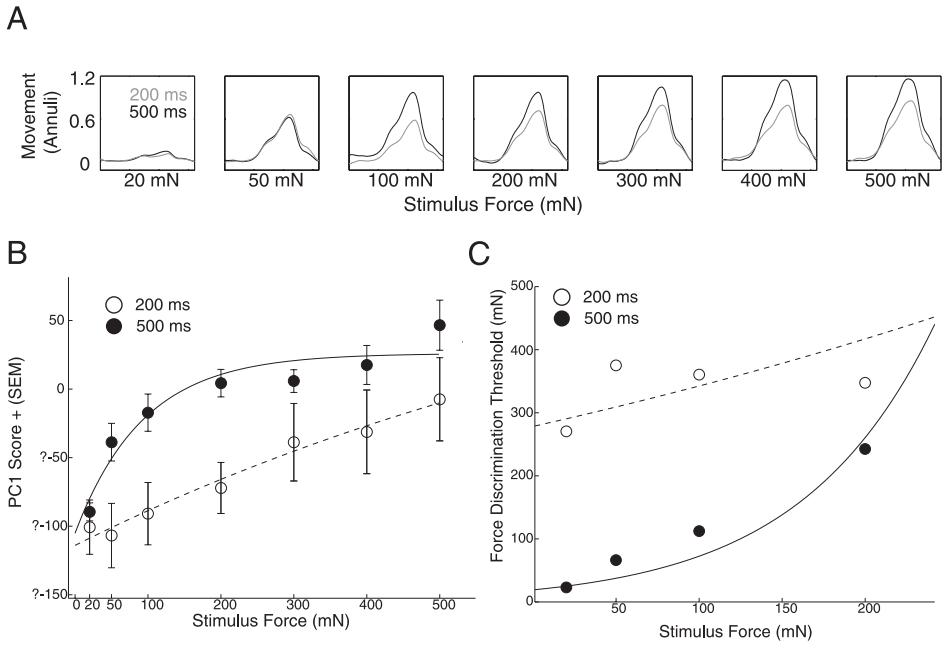

FIG. 6. Stimulus duration affects force discrimination. *A*: we stimulated a body wall at a single location in the ventrolateral territory 10–13 times at 7 different force intensities for 200 and 500 ms. Each plot is an overlay of the means responses to 6 tactile stimuli with durations of 200 ms (gray lines) or 500 ms (black lines). *B*: plot of PC_1 scores as a function of stimulus force for the 2 different stimulus durations. The mean and SE for the PC_1 score are plotted against stimulus force for stimulus durations of 200 and 500 ms in all 6 preparations. Exponential curves are drawn for the 200- and 500-ms groups. For the 500-ms stimuli, the 20-mN force intensity produced a small response that was different from all other responses. The 400- and 500-mN stimuli produced responses that differed from all responses to stimuli ≤100 mN (corrected Tukey-Cramer tests, $P \leq 0.05$). *C*: plots of the force discrimination thresholds, $\Delta_{75}(S)$, generated from data of the sort shown in *A*. The curves fit to the data show that intensity is better discriminated by stimuli with 500-ms durations. For all data in *B* and *C*, $n = 6$.

sensory information must be available to perform a given type of discrimination (Hernandez et al. 1997; Werner 1980). A previous study (Lewis and Kristan 1998a) concluded that touch location was encoded by the P cell responses within 200 ms of stimulus onset: the neuronal encoding of the response was not more accurate with longer stimuli. We found, however, that varying the stimulus duration affected the behavioral discrimination of touch *intensity*. Figure 6*A* shows a representative set of mean bend profiles that were produced by different stimulus intensities and durations for one body-wall preparation. In general, we found that the bend responses generated by stimuli lasting 200 ms were the same shape but smaller than those elicited by 500-ms stimuli of the same intensity. In the three leeches tested, the mean responses to 500-ms stimuli were significantly larger than the responses to 200-ms stimuli at a given intensity except at the very lowest intensities (20 and 50 mN; 2-sided *t*-test, $P \leq 0.01$).

Averaging data across leeches, the responses to 500-ms stimuli have much lower force discrimination thresholds than do the responses to the 200-ms stimuli (Fig. 6*C*). Because the behavior saturates at the higher force intensities, the threshold values approach infinity for both 200- and 500-ms stimuli. However, even at 200 mN, the threshold for the 500-ms stimuli is 100 mN lower than the 200-ms stimuli. These data show that the leech's ability to discriminate touch intensity improves with the 500 as stimulus duration.

DISCUSSION

This study determines some basic psychophysics of the local bending response in the body-wall of the medicinal leech. It asks how far apart two tactile stimuli need to be judged as different, how different two stimulus intensities must be to be judged as different, and how stimulus duration affects intensity judgments. We analyzed these data using a variety of measures, settling on PCA of optical-flow data as the best measures of the localization and the amplitude of stimuli delivered around the circumference of the segmental body-wall. We first measured the distributions of the PCA scores that reproduced the shapes of the bend profiles for each of the stimuli. To determine how finely two stimuli could be discriminated from one another, we used a nearest-neighbor classifier to quantify whether two stimuli were detectably different.

Location discrimination

Using PCA, we calculated the mean threshold for the discrimination of touch location as just under 19°, which corresponds to a distance of 1 mm on a leech with a 2-cm circumference. This is similar to the threshold for discriminating the width of gratings by the human finger tip (~1.0 mm), one of the most sensitive mechanoreceptive regions on the human body (Philips and Johnson 1981). Grating discrimination on the human hand is probably mediated by the slowly adapting (SA) mechanoreceptors because vibrating the gratings to stimulate the rapidly adapting (RA) mechanoreceptors did not significantly improve discrimination. The functional distinctions between RA and SA mechanoreceptors in vertebrates is very similar to the division in leech between rapidly adapting touch mechanoreceptors (T cells) and slowly adapting pressure mechanoreceptors (P cells) (Carlton and McVean 1995; Nicholls and Baylor 1968). The P cells are the major sensory neurons driving the local bend response (Kristan 1982; Lewis and Kristan 1998a; Zoccolan et al. 2002). Hence, similar coding strategies may be used by P cells in leeches and SA mechanoreceptors in vertebrates.

A previous study estimated touch localization in the leech as 28°, using EMG signals to estimate the midpoint of the longitudinal component of the local bend (Lewis and Kristan 1998b). Using these data, the just noticeable difference in touch location would be 38° (applying *Eq. 4* with $m = 1$, assuming response distributions in those studies were Gaussian), an estimate twice the value (18.7°) obtained in this study; this is a significant difference ($P \leq 0.002$, 1-sided *t*-test). There are at least three possible reasons for the different estimates in the two studies. First, EMG is not a reliable indicator of the

total activation of muscles. We abandoned the use of EMGs when, in preliminary experiments, we found that EMG signals were not monotonic functions of motor neuron firing rate (EET, unpublished observations). Second, we obtained a much finer-grained spatial resolution: EMG signals were measured at only four locations (Lewis and Kristan 1998b), whereas our video-based method characterized the bend profiles at 500–640 locations. Third, the previous analysis did not include signals during the 500-ms period of stimulation because that period was thought to be dominated by motor neurons (L cells) that cause bilateral contractions rather than localized bending. It is possible that this initial burst of motor activity should not be ignored.

Intensity discrimination

In the leech mechanosensory system, as in other animals, discriminating between stimulus intensities depends on the absolute intensity of the stimulus. In human psychophysical studies, the relationship between the magnitude of punctate indentation of the skin and the subjective intensity rating reported is often described by a power function (Vega-Bermudez and Johnson 1999). We performed similar analyses in the leech, comparing absolute stimulus intensity to the PC_1 scores that summarize the behavior. We found that a simple exponential function accurately described the relationship between touch intensity and observed behavior. This exponential fit enabled us to compare the absolute stimulus intensity to the threshold intensity increment values [i.e., $\Delta_{75}(I)$]. The observation that the leech discriminates best at lower force intensities and that discriminative ability falls off linearly as the stimulus intensity is increased is similar to other systems where the thresholds [e.g., JNDs or $\Delta_{75}(I)$ values] are proportional to the absolute stimulus intensity (Johnson et al. 1996).

We found that intensity discrimination improves greatly with stimulus duration (Fig. 6*C*), an effect seen in other animals. For instance, to discriminate accurately between mechanically delivered sinusoids that differed only in frequency, monkeys required stimulus durations of ≥250 ms (Hernandez et al. 1997), suggesting to the authors that discriminating the *magnitude* of a sensory input may require different processing than discriminating the *location* of the sensory input. Based on our own and previous work (Lewis and Kristan 1998a), leeches discriminate touch location very well within 200 ms of stimulus onset. However, the ability to discriminate touch intensity with a 200-ms stimulus is improved when the stimulus is presented for 500 ms. The neural underpinning of these different abilities can be further explored by recording from neurons in the local bend network during mechanical stimulation at these different durations.

Limitations of present study

Our methods for quantifying behavioral discrimination of touch location and intensity provide *upper bounds* on how well the leech behaviorally discriminates touch location. It is possible that someone could show, using more precise measures of stimuli, leech behavior or classification algorithms that the leech discriminates better than we have estimated here. In particular, we ignored two aspects of the local bend response in our analysis. First, we did not analyze movement along the circular axis of the body wall. Leeches do display circular movements during local bending (Zoccolan and Torre 2002), and the ventral P cell has a strong synaptic connection to CV, a ventral circular motor neuron (EET, unpublished observation). In this study, we have focused solely on contractions in the longitudinal direction because longitudinal contractions tend to dominate the local bending response (Kristan 1982) and the stimulator arm obstructs the body wall in the location where circular contractions tend to be greatest on the body wall. The second aspect we ignored was the temporal evolution of the local bend response; we analyzed only one time slice from a behavior that lasts many seconds (Fig. 1*G*). It will be an interesting question for future research to determine how the leech's ability to discriminate location and magnitude depends on time.

Comparison of methods for quantifying local bending

We used four methods to summarize the local bend profiles: the maximum, center of mass, cosine fits, and PCA. The goal was to find a method that gave a compact summary of the bend profile that would allow us to quantitatively evaluate how well the leech discriminates touch location and intensity. The maximum was ineffective because each bend profile often had two peaks, and because each peak was at the same location wherever the stimulus was located, the maximum was always at one of these two locations (Fig. 2*B, D* and *F*). The cosine fits provided a poor fit to the data (Fig. 3, *A* and *B*). The center of mass provided a useful measure of the behavior, certainly better than maximum (compare Fig. 2*E* with *D*), but PCA provided both an accurate representation of the entire bend profile (Fig. 3*E*) and was the most sensitive indicator of stimulus location (Fig. 4*D*). We propose that PCA is a very useful measure of behavior of various sorts (D'Avella and Bizzi 1998).

Comparison with previous studies

The present study uses optic flow fields in a different and complementary manner to previous studies (Zoccolan et al. 2001). Previously, the optic flow field was used to construct a six-parameter model of active body-wall deformations, based on linear deformation theory (Giachetti and Torre 1996). This model required each optic flow field to have a single stationary point where no movement occurs. The linear deformation model accounted quite well for movement on small regions of the body wall (Zoccolan et al. 2001). However, when we applied the same model to large regions of the body wall, the fits to the data were not as good. Also, we failed to consistently observe stationary points when we stimulated the body wall mechanically, a necessity for using the linear deformation model. By using PCA, we could look at an optic flow window that spanned the entire circular axis of the leech, allowing us to look at the overall behavior. In both analyses (i.e., linear model or PCA description of behavior), the optic flow algorithm, originally developed for computer vision applications, yields sensitive and quantitative motion estimates that can be related to stimulus parameters.

PCA and implications for the organization of motor output

A previous study used PCA to examine the isometric force fields generated by a single hind limb after stimulating su-

praspinal brain regions in the frog (D'Avella and Bizzi 1998). They observed that five principal components accounted for >95% of the variation in their force field data. They suggested that these five components might correspond to "modules" or building blocks that are consistently co-activated and combine linearly to produce the wiping reflex of the frog's leg. Similarly, just three principal components explained our local bending data and allowed us to characterize the touch and intensity discrimination capacities of the leech. Because the local bend circuitry is well mapped and relatively simple, it is now possible to directly manipulate individual neurons while simultaneously quantifying the changes in behavior using video tracking and PCA. These types of studies should vastly improve our understanding of how sensory information is used to produce behaviors in the leech.

Appendix: derivation of Eq. 4

Assume that two stimuli, s_1 and s_2, are presented with equal likelihood and that each stimulus evokes a Gaussian distribution of responses, $P(R|s_1)$ and $P(R|s_2)$, both with the same SD

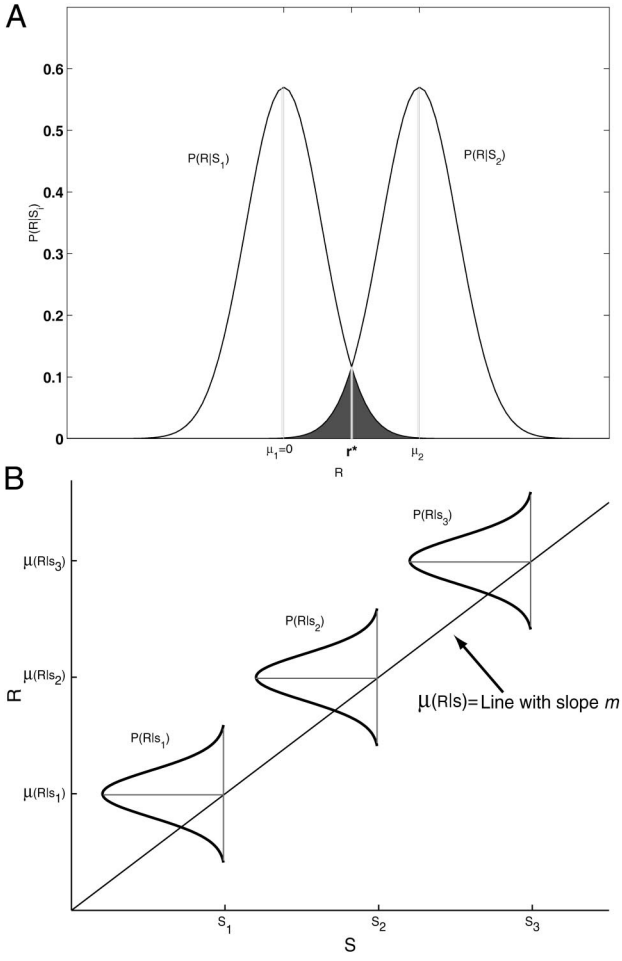

FIG. A1. Derivation of *Eq. 4*. *A*: 2 hypothetical, identical Gaussian distributions of responses, $P(R|s_1)$ and $P(R|s_2)$, to 2 stimuli, s_1 and s_2. r^* is the *decision boundary value* used by a maximum likelihood decoder to "decide" whether s_1 was presented (if $R < r^*$) or s_2 was presented (if $R > r^*$). *B*: theoretical input/output function in which a Gaussian response with mean $\mu_{R|S}$ is evoked by stimulus *S*, and $\mu_{R|S}$ increases linearly with *S*. Three of the response distributions (to arbitrary stimuli s_1–s_3) are shown for illustrative purposes. The SD σ_s of the response at each *S* is assumed to be the same.

σ_R but with different means $\mu_1 = 0$ and μ_2, respectively (Fig. A1*A*). (Setting μ_1 to 0 does not affect the generality of the results that follow, but serves to simplify the calculations.)

Given these assumptions, the performance of an *ideal observer*, also called a *minimum error classifier* (Duda et al. 2000), is achieved by following the *maximum likelihood rule*: given a response r from the set of all possible responses R, classify r as being evoked by the stimulus s_i such that $P(r|s_i) > P(r|s_j)$. The maximum likelihood rule generates a decision boundary, r^* (Fig. A1*A*), which is the value of R above which s_2 is chosen and below which s_1 is chosen (Duda et al. 2000). r^* is the value half-way between the peaks of the two response distributions; it marks the value at which the classifier operates at chance performance (i.e., 50% correct). Because r^* lies halfway between μ_1 and μ_2, it follows that $\mu_2 = 2r^*$. The probability of a classification error is the area of overlap under the curves $0.5P(R|s_1)$ and $0.5P(R|s_2)$, which is the shaded region in Fig. A1*A* (Thomson and Kristan 2005). Therefore determining $\Delta_{75}(\mu_{R|s})$, the distance between the means of the two distributions at which an ideal observer would perform at 75% correct, is reduced to finding the distance, $2r^*$, at which the area of overlap is 25% of the total area.

The value of R beyond which 12.5% of the area in $P(R|s_1)$ lies (i.e., $r_{.125}$) is determined by

$$\int_{r_{0.125}}^{\infty} \frac{1}{2} P(R|S_1) = 0.125 \qquad (A1)$$

If $P(R|s_1)$ is Gaussian, as we are assuming, then the solution to *Eq. A1* is

$$r_{0.125} = \text{cumgauss}^{-1}(0.75, \sigma_R) \qquad (A2)$$

where $\text{cumgauss}^{-1}(p,\sigma_R)$, denotes the inverse cumulative distribution function of a Gaussian with SD σ_R and a mean of 0 (Larsen and Marx 2000). In a system with a decision boundary value r^* equal to $r_{0.125}$, the contribution that $P(R|s_1)$ makes to the area of overlap between $P(R|s_1)$ and $P(R|s_2)$ is the area located to the right of r^*, an area that we chose to be 0.125. Because $P(R|s_1)$ and $P(R|s_2)$ are symmetric about r^*, $P(R|s_2)$ contributes the same overlap area to the *left* of r^*. The *sum* of the contributions of $P(R|s_1)$ and $P(R|s_2)$ is 0.25, which is the overlap at threshold we are seeking. Hence, the distance between the means of the Gaussians at threshold is

$$\Delta_{75}(\mu_{R|s}) = 2r^* = 2\text{cumgauss}^{-1}(0.75, \sigma_R) \qquad (A3)$$

Using *Eq. A3,* if we have an estimate of σ_R, we can calculate $\Delta_{75}(\mu_{R|s})$. However, $\Delta_{75}(\mu_{R|s})$ measures how far apart two distributions must be in *response* space, whereas the goal is to calculate the corresponding distance in *stimulus* space, $\Delta_{75}(S)$, which would *produce* response means separated by $\Delta_{75}(\mu_{R|s})$. To calculate $\Delta_{75}(S)$, we first assume that the response mean changes linearly with the stimulus. That is

$$\mu_{R|s} = ms \qquad (A4)$$

where $\mu_{R|s}$ is the expected value of R in response to stimulus s, and m is the slope of the line relating the variables. Figure A1*B* illustrates this assumption: for each stimulus, there is a Gaussian distribution of responses, and as the stimulus value increases, the mean of the corresponding Gaussian increases linearly. From *Eq. A4,* it follows that $\Delta_{75}(\mu_{R|s})/\Delta_{75}(S) = m$, so

$$\Delta_{75}(S) = \Delta_{75}(\mu_{R|s})/m = 2\text{cumgauss}^{-1}(.75, \sigma_R)/m \quad (A5)$$

where the second equality is obtained by the use of *Eq. A3*. This is *Eq. 4,* the equation we intended to prove.

ACKNOWLEDGMENTS

We thank D. Zoccolan for advice about optic flow and for providing data so that we could compare optic flow algorithms, Dr. Ming Ye for advice and for allowing us to use her optic flow code, Dr. Eduardo J. Chichilnisky for pointing out the utility of principal component analysis, and Dr. Geoff Chander for assistance with modifying the dual-mode lever system that was used for stimulating the body wall.

GRANTS

This work was funded by National Institutes of Health Grants MH-43396 and NS-35336 to W. B. Kristan, by a Merck and Predoctoral Fellowhip GM-08107 to E. E. Thomson, and by a Merck and a National Research Service Award MH-13037 to S. M. Baca.

REFERENCES

Andrews K. The effect of changes in temperature and humidity on the accuracy of von Frey hairs. *J Neurosci Methods* 50: 91–93, 1993.

Badcock DR and Schor CM. Depth-increment detection function for individual spatial channels. *J Opt Soc Am A* 2: 1211–1216, 1985.

Barron JL, Fleet DJ, and Beauchemin SS. Performance of optical flow techniques. *Int J Comp Vis* 12: 43–77, 1994.

Beauchemin SS and Barron JL. The computation of optical flow. *ACM Comput Surveys* 27: 433–467, 1995.

Bergen, JR, Anandan P, Hanna, KJ and Hingorani R. Hierarchical model-based motion estimation. *Eur Conf Comp Vis* 588: 237–252, 1992.

Buzuloiu V, Ciuc M, Rangayyan RM, and Vertan C. Adaptive-neighborhood histogram equalization of color images. *J Electr Imag* 10: 445–459, 2001.

Carlton T and McVean A. The role of touch, pressure, and nociceptive mechanoreceptors of the leech in unrestrained behavior. *J Comp Physiol [A]* 177: 781–791, 1995.

Churchland PS and Sejnowski TJ. *The Computational Brain.* Cambridge, MA: MIT Press, 1992.

D'Avella A and Bizzi E. Low dimensionality of supraspinally induced force fields. *Proc Natl Acad Sci USA* 95: 7711–7714, 1998.

Duda RO, Hart PE, and Stork HG. *Pattern Classification* (2 ed.). New York: Wiley-Interscience, 2000.

Giachetti A and Torre V. The use of optical flow and for the analysis of non-rigid motions. *Int J Comput Vision* 18: 255–279, 1996.

Hernandez H, Salinas E, Garcia R, and Romo R. Discrimination in the sense of flutter: new psychophysical measurements in monkeys. *J Neurosci* 17: 6391–6400, 1997.

Jackson EJ. *A User's Guide to Principal Components.* New York: Wiley, 1991.

Johnson KO and Philips JR. Tactile spatial resolution. I. Two-point discrimination, gap detection, grating resolution, and letter recognition. *J Neurophysiol* 46: 1177–1191, 1981.

Johnson KO, Steven HS, and Blake DT. Linearity as the basic law of psychophysics: Evidence from studies of the neural mechanisms of roughness magnitude estimation. In: *Somasthesis and the Neurobiology of the Somatosensory Cortex*, edited by Franzen O. and Terenius. Basel, Switzerland: Birkhauser Verlag, 1996.

Kristan WB. Sensory and motor neurones responsible for the local bending response in leeches. *J Exp Biol* 96: 161–180, 1982.

Larsen RJ and Marx ML. *An Introduction to Mathematical Statistics and its Applications* (3rd ed.). Englewood Cliffs, NJ: Prentice Hall, 2000.

Lewis JE. Sensory processing and the network mechanisms for reading neuronal population codes. *J Comp Physiol [A]* 185: 373–378, 1999.

Lewis JE and Kristan WB Jr Representation of touch location by a population of leech sensory neurons. *J Neurophysiol* 80: 2584–2592, 1998a.

Lewis JE and Kristan WB Jr Quantitative analysis of a directed behavior in the medicinal leech: implications for organizing motor output. *J Neurosci* 18: 1571–1582, 1998b.

Lewis JE and Kristan WB Jr. A neuronal network for computing population vectors in the leech. *Nature* 391: 76–79, 1998c.

Lockery SR and Kristan WB Jr. Distributed processing of sensory information in the leech. I. Input-output relations of the local bending reflex. *J Neurosci* 10: 1811–1815, 1990a.

Lockery SR and Kristan WB Jr. Distributed processing of sensory information in the leech. II. Identification of interneurons contributing to the local bending reflex. *J Neurosci* 10:1816–1829, 1990b.

Lockery SR and Kristan WB Jr. Two forms of sensitization of the local bending reflex of the medicinal leech. *J Comp Physiol [A]* 108: 165–177, 1991.

Lucas BD and Kanade T. An iterative image registration technique with an application to stereo vision (IJCAI). In: *Proceedings of the 7th International Joint Conference on Artificial Intelligence.* San Francisco: Morgan Kaufmann, 1981, p. 674–679.

Mason A and Kristan WB Jr. Neuronal excitation, inhibition, and modulation of leech longitudinal muscle. *J Comp Physiol* 146: 527–536, 1982.

Morrow WM, Paranjape RB, Rangayyan RM, and Desautels JEL. Region-based contrast enhancement of mammograms. *IEEE Trans Med Imag* 11: 392–406, 1992.

Muller KJ, Nicholls JG, and Stent GS. Appendix C: The nervous system of the leech: a laboratory manual. In: *Neurobiology of the Leech*. New York: Cold Spring Harbor Laboratory, 1981, p. 249–275.

Nicholls JG and Baylor DA. Specific modalities and receptive fields of sensory neurons in CNS of the leech. *J Neurophysiol* 31: 740–756, 1968.

Paranjape RB, Morrow WM, and Rangayyan RM. Adaptive-neighborhood histogram equalization for image enhancement. *CVGIP: Graph Mod Image Proc* 54: 259–267, 1992.

Paranjape RB, Rangayyan RM, and Morrow WM. Adaptive neighborhood mean and median image filtering. *J Elect Imag* 3: 360–367, 1994.

Parker AJ and WT Newsome Sense and the single neuron: probing the physiology of perception. *Annu Rev Neurosci* 21: 227–277, 1998.

Philips JR and Johnson KO. Tactile spatial resolution. II. Neural representation of bars, edges, and gratings in monkey primary afferents. *J Neurophysiol* 46: 1192–1203, 1981.

Pinato G and Torre V. Coding and adaptation during mechanical stimulation in the leech nervous system. *J Physiol* 529: 747–762, 2000.

Sekular R and Blake R. *Perception.* New York: McGraw-Hill, 1990

Stuart AE. Excitatory and inhibitory motoneurons in the central nervous system of the leech. *Science* 165: 817–819, 1969.

Stuart AE. Physiological and morphological properties of motoneurones in the central nervous system of the leech. *J Physiol* 209: 627–646, 1970.

Thomson EE and Kristan WB Jr. Quantifying stimulus discriminability: a comparison of information theory and ideal observer analysis. *Neural Comput* 17: 741–778, 2005.

Vega-Bermudez F and Johnson KO. SA1 and RA receptive fields, response variability, and population responses mapped with a probe array. *J Neurophysiol* 81: 2701–2710, 1999.

Werner G. The study of sensation in physiology. In: *Medical Physiology*, edited by Mountcastle VB. St. Louis, MO: Mosby, 1980, vol. 1, p. 605–628.

Ye M and Haralick RM. Image flow estimation using facet model and covariance propagation. In: *Vision Interface: Real World Applications of Computer Vision,* edited by Cheriet M and Yang YH. Hackensack, NJ: World Scientific 2000, vol. 35, p. 209–241.

Zar JH. *Biostatistical Analysis.* Englewood Cliffs, NJ: Prentice Hall, 1999.

Zoccolan D, Giachetti A, and Torre V. The use of optical flow to characterize muscle contraction. *J Neurosci Methods* 110: 65–80, 2001.

Zoccolan D, Pinato G, and Torre V. Highly variable spike trains underlie reproducible sensorimotor responses in the medicinal leech. *J Neurosci* 22: 10790–10800, 2002.

Zoccolan D and Torre V. Using optical flow to characterize sensory-motor interactions in a segment of the medicinal leech. *J Neurosci* 22: 2283–2298, 2002.